Thermodynamics of Temperature-Sensitive Polyether-Modified Poly(acrylic acid) Microgels

Lev Bromberg, Marina Temchenko, Geoffrey D. Moeser, and T. Alan Hatton*

Department of Chemical Engineering, Massachusetts Institute of Technology, Cambridge, Massachusetts 02139

Received October 20, 2003. In Final Form: March 5, 2004

The temperature-induced structural changes and thermodynamics of ionic microgels based on poly(acrylic acid) (PAA) networks bonded with poly(ethylene oxide)-*b*-poly(propylene oxide)-*b*-poly(ethylene oxide) (PEO−PPO−PEO) (Pluronic) copolymers have been studied by small-angle neutron scattering (SANS), ultra-small-angle neutron scattering (USANS), differential scanning calorimetry (DSC), and equilibrium swelling techniques. Aggregation within microgels based on PAA and either the hydrophobic Pluronic L92 (average composition, $EO_8PO_{52}EO_8$; PPO content, 80%) or the hydrophilic Pluronic F127 (average composition, $EO_{99}PO_{67}EO_{99}$; PPO content, 30%) was studied and compared to that in the solutions of the parent Pluronic. The neutron scattering results indicate the formation of micelle-like aggregates within the F127-based microgel particles, while the L92-based microgels formed fractal structures of dense nanoparticles. The microgels exhibit thermodynamically favorable volume phase transitions within certain temperature ranges due to reversible aggregation of the PPO chains, which occurs because of hydrophobic associations. The values of the apparent standard enthalpy of aggregation in the microgel suspensions indicate aggregation of hydrophobic clusters that are more hydrophobic than the un-cross-linked PPO chains in the Pluronic. Differences in the PPO content in Pluronics L92 and F127 result in a higher hydrophobicity of the resulting L92−PAA−EGDMA microgels and a larger presence of hydrophobic, densely cross-linked clusters that aggregate into supramolecular structures rather than micelle-like aggregates such as those formed in the F127−PAA−EGDMA microgels.

Introduction

The field of microgels, that is, cross-linked latex particles of submillimeter size that can be swollen in a good solvent, is rapidly expanding to include nanosized gels as well as so-called smart microgels that undergo volume phase transitions in response to changes in the solvent quality.[1−4] Aqueous microgels are an integral part of important water-borne polymer technologies used in the industrial processing industries, cosmetics, coatings, food, consumer products, and pharmaceutical formulations. The majority of the microgels that swell and collapse by absorbing or expelling water, respectively, in response to the temperature changes in their environment have been based on poly(*N*-isopropylacrylamide) or related *N*-alkylacrylamides[4] and, less frequently, poly(*N*-vinyl caprolactam), poly(vinyl methyl ether), and a few other amphiphilic polymers with a lower critical solution temperature (LCST) in water.[5,6] We have recently introduced a new family of hydrophobically modified polyelectrolytes that incorporate poly(propylene oxide) (PPO) as one of their structural components and thus inherit the limited, temperature-sensitive solubility of PPO in water.[7−14] In these copolymers, poly(ethylene oxide)-*b*-poly(propylene oxide)-*b*-poly(ethylene oxide) (PEO−PPO−PEO) copolymers are covalently bonded with multiple poly(acrylic acid) (PAA) segments, typically resulting in long (MW > 10^5 Da), temperature- and pH-sensitive graft-comb copolymers. These copolymers, often abbreviated as Pluronic−PAAs, are effective rheology modifiers capable of forming viscoelastic physical gels in semidilute solutions.[8,9,11] The Pluronic−PAAs are benign, nonirritating, and form micelle-like aggregates, which are all properties useful in biomedical applications.[15] The introduction of a divinyl cross-linker in the process of the synthesis of Pluronic−PAA resulted in the advent of new thermosensitive microgels,[16,17] the morphology of which can be tailored by utilization of Pluronic copolymers with varying compositions.

In the present study, we concentrated on the temperature-dependent structural features and thermodynamic properties of the novel Pluronic−PAA microgels that appear to be quite different in their swelling behaviors and structures, depending on the Pluronic used in the synthesis of the copolymers.[17] We conducted a comparative study of the microgels (using neutron scattering and differential scanning calorimetry) and aqueous solutions of their parent Pluronic copolymers, for which the thermodynamic properties are well-documented.[18−25]

(1) Murray, M. J.; Snowden, M. J. *Adv. Colloid Interface Sci.* **1995**, *54*, 73.
(2) Saunders, B. R.; Vincent, B. *Adv. Colloid Interface Sci.* **1999**, *80*, 1.
(3) Funke, W.; Okay, O.; Joos-Müller, B. *Adv. Polym. Sci.* **1998**, *136*, 139.
(4) Pelton, R. *Adv. Colloid Interface Sci.* **2000**, *85*, 1.
(5) Viholaa, H.; Laukkanen, A.; Hirvonena, J.; Tenhu, H. *Eur. J. Pharm. Sci.* **2002**, *16*, 69.
(6) Schäfer-Soenen, M.; Moerkerke, R.; Koningsveld, R.; Berghmans, H.; Dušek, K. Šolc, K. *Macromolecules* **1997**, *30*, 410.
(7) Bromberg, L. *J. Phys. Chem. B* **1998**, *102*, 1956.
(8) Bromberg, L. *Macromolecules* **1998**, *31*, 6148.
(9) Bromberg, L. *Langmuir* **1998**, *14*, 5806.
(10) Bromberg, L. *Ind. Eng. Chem. Res.* **1998**, *37*, 4267.
(11) Bromberg, L. *J. Phys. Chem. B* **1998**, *102*, 10736.
(12) Bromberg, L. E.; Barr, D. P. *Macromolecules* **1999**, *32*, 3649.
(13) Huibers, P. D. T.; Bromberg, L. E.; Robinson, B. H.; Hatton, T. A. *Macromolecules* **1999**, *32*, 4889.
(14) Bromberg, L. *Ind. Eng. Chem. Res.* **2001**, *40*, 2437.
(15) Bromberg, L. In *Handbook of Polyelectrolytes and Their Applications*; Tripathy, S., Nalwa, H. S., Eds.; American Scientific Publishers: Stevenson Ranch, CA, 2002; Chapter 2.
(16) Bromberg, L.; Temchenko, M.; Hatton, T. A. *Langmuir* **2002**, *18*, 4944.
(17) Bromberg, L.; Temchenko, M.; Hatton, T. A. *Langmuir* **2003**, *19*, 8675.
(18) Hecht, E.; Hoffmann, H. *Colloids Surf., A* **1995**, *96*, 181.
(19) Alexandridis, P.; Hatton, T. A. *Colloids Surf., A* **1995**, *96*, 1.

10.1021/la0359530 CCC: $27.50 © 2004 American Chemical Society
Published on Web 06/05/2004

Table 1. Composition and Ion-Exchange Properties of Microgels

parameter	F127−PAA− EGDMA	L92−PAA− EGDMA
content, g/g dry	0.55	0.55
PAA		
PPO	0.15	0.36
PEO	0.30	0.09
EGDMA	0.015	0.015
total ion-exchange capacity, meq/g dry	6.12	7.23
intrinsic dissociation constant, pK_0	4.95	6.27

Experimental Section

Materials. Pluronic, triblock copolymers of ethylene oxide (EO) and propylene oxide (PO) were obtained from BASF (Mount Olive, NJ) and were chosen to represent the hydrophobic Pluronic L92 (average composition, $EO_8PO_{52}EO_8$) and the relatively hydrophilic Pluronic F127 (average composition, $EO_{99}PO_{67}EO_{99}$) extremes of this class of block copolymers. The microgels were synthesized by emulsion/dispersion copolymerization of the Pluronic and acrylic acid, using ethylene glycol dimethacrylate (EGDMA) as a cross-linker. The procedures of the microgel particle synthesis and purification have been described in detail previously.[16] The weight ratio of the Pluronic to poly(acrylic acid) in the microgels was set at 45:55, and the molar ratio of the EGDMA to acrylic acid was set at 1 mol %. The composition and properties of the microgels were characterized by the previously described[17] titration method and are collected in Table 1.

Methods. Neutron Scattering Experiments. Small-angle neutron scattering (SANS) experiments were carried out on the LOQ instrument at ISIS (Rutherford Appleton Laboratory, U.K.). This instrument uses a neutron beam with a wavelength (λ) range from 2.2 to 10 Å. The 64 cm × 64 cm detector was fixed at a distance of 4.1 m from the sample. A disk chopper was combined with time-of-flight analysis to resolve neutrons of different wavelengths. This, combined with measurements of sample transmission, background, and empty cell scattering, was used to provide measurements of scattering intensity on an absolute scale that spanned a $0.0073\ Å^{-1} < q < 0.23\ Å^{-1}$ range. The scattering vector (q) is defined as $(4\pi/\lambda)\sin(\theta/2)$, where θ is the angle between the beam and the scattered neutron. To prepare samples for SANS analysis, microgel samples were dried and then dissolved in D_2O at 2 wt %. The samples were then neutralized with NaOD solution. All measurements were conducted in circular cells with a 5 mm path length. The temperature of the sample cells was varied from 10 to 50 °C using an external water bath circulator.

Ultra-small-angle neutron scattering (USANS) measurements were performed on a BT5 USANS perfect crystal defractometer at the National Institute of Standards and Technology Center for Neutron Research (Gaithersburg, MD). A premonochromator and Si(220) monochromator were used to select a neutron beam with a wavelength of 2.4 Å that was directed at the sample. The transmitted beam and scattered neutrons were directed into a matching Si(220) analyzer crystal that was rotated by an angle of θ to guide neutrons scattered by angle q to the detector. Varying the angle of the analyzer resulted in a useable q range of $4.0 \times 10^{-5}\ Å^{-1} < q < 0.0044\ Å^{-1}$. The scattering intensity was corrected for transmission by subtracting the intensity of beam scattering at $q = 0$. The background scattering was corrected by measuring the scattering intensity of the solvent, and the data were placed on an absolute background. A correction for slit smearing (due to scattering in the vertical direction that was not selected by the analyzer) was performed using software supplied by NIST. USANS samples were prepared by a procedure identical to that used for SANS analysis. All measurements were conducted in circular cells with a 7 mm path length, and the temperature of the sample cells was varied from 10 to 50 °C using an external water bath circulator.

Calorimetry Study. The particles were dispersed in deionized water at a known concentration and were allowed to equilibrate at 4−8 °C for 2 days. To ensure the absence of unattached Pluronic admixtures, a gel fraction that was subsequently used in the calorimetry experiments was exhaustively dialyzed (membrane molecular weight cutoff, 30 kDa) against excess deionized water (pH adjusted to 7.0) at 4−8 °C for 1 week, followed by lyophilization. The lyophilized samples were reconstituted with deionized water and allowed to equilibrate at 4−8 °C for at least 48 h, followed by pH adjustment prior to the calorimetric experiments.

A micro DSC III instrument (SETARAM, France) with an ultralow background noise (<0.2 μW) was employed in the conventional differential scanning calorimetry (DSC) measurements. The liquid samples weighing 70−100 mg were placed in a fluid-tight batch vessel and run against deionized water (pH adjusted to 7.0) as a reference. Multiple heating−cooling cycling scans were performed with scan rates of 1 K/min, unless indicated otherwise. The heat flow versus temperature signal was used to obtain the maximum peak temperature (T_m). Using the PeakFit Version 4.11 (SYSTAT, Inc., Richmond, CA) software, all thermograms were fitted by a linear baseline calculated using the entire temperature range and then subtracted from the signal. Using the third heating endotherm (see the Results and Discussion section below), the reproducibility of the T_m determination was found to be ±0.1 K in three independent measurements.

A DSC Q1000 instrument (TA Instruments, New Castle, DE) equipped with a refrigerated cooling system and advanced Tzero technology was used for the heat capacity measurements. Microgel suspensions or polymer solutions weighing in the range 11−17 mg were sealed in aluminum pans. The mass of the samples was low enough to allow the sample to follow the imposed thermal oscillations.[26,27] The temperature and the enthalpy were calibrated using indium as a standard, the baseline was calibrated by scanning the temperature domain (278−333 K) with an empty pan, and the modulus of the complex heat capacity was calibrated by the measurement of sapphire in the studied temperature range at the lowest frequency allowed by the instrument. In a typical experiment, a sample was first subjected to two consecutive heating−cooling scans at a constant 1 K/min rate in a conventional DSC mode. The width of the transition peak was estimated, and the instrument's built-in software was used to set the frequency of the subsequent modulated DSC (MDSC) run such that the modulated heat flow exhibited four to six cycles over the transition width at $^1/_2$ of the peak height (Figure 1). In an MDSC run, the instantaneous heating rate is given by[28]

$$\frac{dT}{dt} = \beta + A_T\omega\cos\omega t \qquad (1)$$

The preset parameter values were typically as follows: underlying heating rate, $\beta = 0.0167$ K/s; amplitude, $A_T = \pm 0.16$ K; and frequency, $\omega = 0.1$ rad/s.

The total heat flow signal was analyzed in terms of the reversing heat capacity component (C_p) and the nonreversing (kinetic) enthalpic recovery:[28,29]

$$\frac{dQ}{dt} = C_p\frac{dT}{dt} + f(T, t) \qquad (2)$$

where Q is the heat energy and $f(T, t)$ is the calorimetric response to any kinetically controlled phenomena. The component representing the second term in eq 2 was featureless, sometimes deviating from linearity well above the pronounced peak exhibited by the reversing C_p component (Figure 1). The maximum of this peak coincided, within ±1 K, with the T_m value measured by the

(20) Patterson, I.; Chowdhry, B. Z.; Leharne, S. *Colloids Surf., A* **1996**, *111*, 213.
(21) Almgren, M.; Brown, W.; Hvidt, S. *Colloid Polym. Sci.* **1995**, *273*, 2.
(22) Chu, B.; Zhou, Z. *Surfactant Sci. Ser.* **1996**, *60*, 67.
(23) Alexandridis, P. *Curr. Opin. Colloid Interface Sci.* **1997**, *2*, 478.
(24) Wanka, G.; Hoffmann, H.; Ulbricht, W. *Macromolecules* **1994**, *27*, 4145.
(25) Alexandridis, P.; Holzwarth, J. F. *Langmuir* **1997**, *13*, 6074.
(26) Schawe, J. E. K.; Winter, W. *Thermochim. Acta* **1997**, *298*, 9.
(27) Bustin, O.; Descamps, M. *J. Chem. Phys.* **1999**, *110*, 10982.
(28) Jiang, Z.; Imrie, C. T.; Hutchinson, J. M. *Thermochim. Acta* **2002**, *387*, 75.
(29) Coleman, N. J.; Craig, D. Q. M. *Int. J. Pharm.* **1996**, *135*, 13.

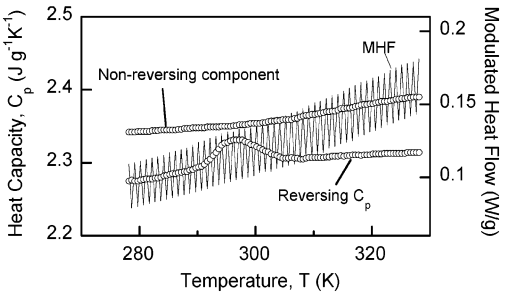

Figure 1. Modulated DSC (MDSC) heating scan of a 1 wt % aqueous suspension of the L92−PAA−EGDMA microgel (pH 7.0). The MDSC was run following two heating−cooling DSC scans. The open points show the reversing (circles) and nonreversing (diamonds) heat capacity data; the solid line represents the modulated heat flow (MHF). Underlying heating rate, 0.0167 K/s; amplitude, ±0.16 K; frequency, 0.1 rad/s. Every tenth point of the heat capacity data is shown for clarity.

conventional DSC method. To obtain calorimetric values of the enthalpy (ΔH_{cal}) and entropy (ΔS_{cal}) of the transition, the experimental thermograms were integrated throughout the temperature range of the peak:

$$\Delta H_{cal} = \int C_p(T)\, dT \qquad \Delta S_{cal} = \int C_p(T)\, d \ln T \quad (3)$$

The ΔH_{cal} values obtained in this way coincided, within ±5%, with the enthalpy values obtained by integrating the heat flow signal in the corresponding conventional DSC runs. The temperature of transition obtained from the integrated thermograms ($T_{tr} = \Delta H_{cal}/\Delta S_{cal}$) coincided, within ±0.2%, with the T_m values obtained from the C_p versus T peak maxima.

Microgel Swelling Experiments. The ability of microgels to absorb water was studied using a volumetric method. Single microgel particles pre-equilibrated in deionized water at 4−8 °C were placed into glass capillary tubes (internal diameter, 1−1.2 mm) using suction pressures applied by an Ultramicro Accropet filler/dispenser (Carolina Biological Supply Company, Burlington, NC) via a rubber connector. The tubes were placed into a homemade glass thermostated cuvette and observed under a Nikon TMS inverted microscope (Nikon Corp., Tokyo, Japan) equipped with a model IV-550 video microscaler (For-A Co., Tokyo, Japan) and a Hitachi color video monitor. The boundaries of the spherical particles were fit with the microscaler, and the particle diameter was measured with an accuracy of ±0.5 μm or better. Initially, the diameter of a particle swollen at a reference temperature (d_0) was measured. The capillary tube was then equilibrated at a different temperature. The diameter of the swollen particle (d_t) was measured for 20−30 min until no further changes in d_t were observed. In a control series of experiments, changes in d_t/d_0 upon increasing temperature were recorded and compared to those with the same microgel particle upon decreasing temperature. A hysteresis of ∼10−15% of the maximum d_t/d_0 value was observed. However, upon a subsequent second heating, the d_t/d_0 versus T data coincided with those obtained upon the previous cooling, indicating that the equilibrium state was attained at the first cooling. Thus, all the swelling experiments were performed using a heating−cooling cycle and the results of the cooling/equilibration experiment are reported below. Measurements at pH 7.0 over a given temperature range were conducted with three to five different particles in different capillary tubes.

Results and Discussion

Neutron Scattering Study. The scattering data from the SANS and USANS measurements are presented on the same scale in Figure 2 for the Pluronic−PAA−EGDMA microgels at four temperatures spanning a 10−50 °C range. There is a small q-range gap (0.0044 Å^{-1} < q < 0.0073 Å^{-1}) in the data due to the instrument configurations used in these experiments. The SANS and USANS scattering curves for the F127−PAA−EGDMA microgels

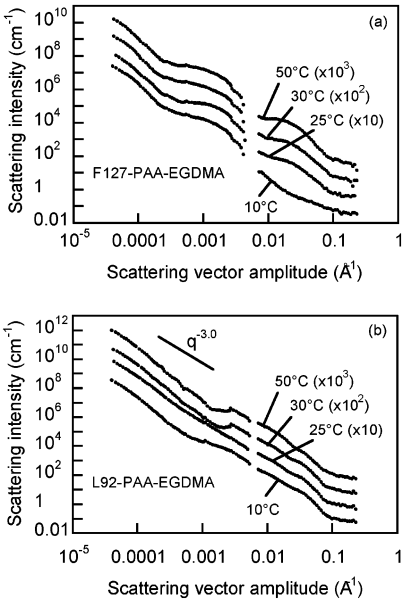

Figure 2. Scattering curves for 2 wt % aqueous dispersions of the (a) F127−PAA−EGDMA and (b) L92−PAA−EGDMA microgels (pH 7.0).

in Figure 2a appear to mesh well at all temperatures if the USANS data are extrapolated to the SANS q range. These data required no scaling, indicating that the absolute intensity of both the SANS and USANS data was correct. The scattering data for the L92−PAA−EGDMA microgels in Figure 2b, on the other hand, required that the USANS data be multiplied by a scale factor of ∼5 for the data to mesh. This scaling was required because the L92−PAA−EGDMA concentration decreased during the USANS run due to settling; no such settling of the F127−PAA−EGDMA particles was observed, as this suspension was significantly more viscous. We hypothesize that the offset between the SANS and USANS data is a result of the desmearing algorithm used for the USANS data to account for slit smearing effects. In the case of the L92−PAA−EGDMA microgel, this procedure forced a power law decay of the USANS data at the upper end of its q range. Some of the L92−PAA−EGDMA microgel scattering curves (such as at 30 and 50 °C) were beginning to level out in this range, so the desmearing algorithm may have resulted in an offset of the L92−PAA−EGDMA microgel USANS data. Desmearing did not cause difficulties in interpretation of the F127−PAA−EGDMA microgel data.

The primary difference in the scattering data between the F127−PAA−EGDMA and L92−PAA−EGDMA microgels is seen in the SANS region (0.0073 Å^{-1} < q < 0.23 Å^{-1}). Here, the scattering curves for the F127−PAA−EGDMA samples (Figure 2a) show a significant difference as the temperature is varied between 10 and 50 °C, while the L92−PAA−EGDMA scattering (Figure 2b) shows almost no change. Previous studies of Pluronic−PAA polymers that were not cross-linked by EGDMA have indicated that micelle-like structures may exist in these systems at certain temperatures.[13] If we assume that similar spherical particles are the cause of scattering in the SANS region for these microgels, we can express the intensity of the scattered neutrons ($I(q)$) as

$$I(q) = \phi(\Delta\rho)^2 VP(q, R)S(q, R, \phi) \quad (4)$$

where ϕ is the volume fraction of the particles, $\Delta\rho$ is the scattering length density contrast between the particles

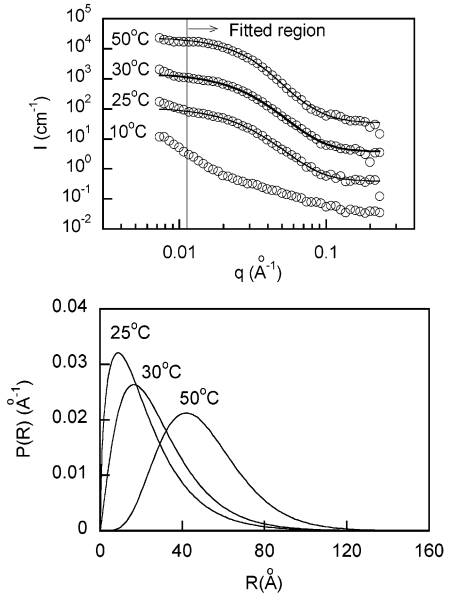

Figure 3. (a) Scattering in the SANS region for the F127−PAA−EGDMA microgels. The solid lines represent the best fit to the data with a model for polydisperse spheres. (b) Size distribution of the spherical particles as determined by the best fit to the SANS data.

and the bulk, V is the particle volume, and R is the radius. The normalized form factor $P(q, R)$ is a function of the particle size and shape, while the structure factor $S(q, R, \phi)$ is a result of interactions between particles.

The experimental scattering of F127−PAA−EGDMA in the SANS region is shown in more detail in Figure 3a. At the three higher temperatures, the curves show an upturn at very low q values (<0.01 Å^{-1}), which continues into the USANS region, as shown in Figure 2a. Thus, we limited our fit of the SANS data to the region $q > 0.11$ Å^{-1} because it appears that scattering above this limit is due primarily to intraparticle effects (as shown by the leveling off of the data above this point) and therefore neglected interparticle interactions by setting $S(q, R, \phi) = 1$. The form factor was calculated by assuming that the particles were polydisperse spheres, with the polydispersity given by a Schultz distribution:

$$p(R) = \frac{1}{\Gamma(Z+1)}\left(\frac{Z+1}{R_0}\right)^{Z+1} R^Z \exp\left[-\frac{(Z+1)R}{R_0}\right] \quad (5)$$

where R_0 is the average radius and Z is a width parameter that is more clearly described by the root-mean-square deviation of the distribution: $\sigma = R_0/(Z+1)^{1/2}$.[30,31] With this distribution of spherical particles, an analytical solution for the form factor exists, details of which can be found in the literature.[30,31] This model for scattering has been successfully applied to many colloidal systems.[30−34]

The best fit to the F127−PAA−EGDMA data with this model (in the SANS region) is shown in Figure 3a as the solid lines. For each data series, there are three fitted parameters, R_0, σ/R_0, and $\phi(\Delta\rho)^2$. We note that we cannot independently determine ϕ and $\Delta\rho$, as it is uncertain what fraction of the polymer in the microgel participates in domain formation and what fraction of water is present in these domains. For the F127−PAA−EGDMA microgel at 10 °C, we were unable to fit the data with a model for polydisperse spheres. However, at 25 °C and higher temperatures, a very good fit to the data was achieved. The values of the best-fit parameters are given in Table 2, which shows that, as the temperature is increased above 25 °C, the size of the domains becomes larger, while the distribution becomes relatively narrower; this is also shown in Figure 3b, which illustrates the predicted size distributions of the domains from the SANS analysis. The predicted value of the $\phi(\Delta\rho)^2$ scale factor in Table 2 is reasonable, since assuming that $\Delta\rho = 3.0 \times 10^{-10}$ cm^{-2} (a representative value for D_2O swollen particles), this yields a ϕ value of 0.7−1.2% (including any solvent present in the domains). This result compares well with a total microgel volume fraction of 2.0%, which suggests that a significant part of the microgel is not present in the domains.

Table 2. Fitted Parameters, R_0, σ/R_0, and $\phi(\Delta\rho)^2$, Obtained from SANS Data for the F127−PAA−EGDMA Microgels in the Temperature Range 25−50 °C[a]

T, °C	R_0, A	σ/R_0	$\phi(\Delta\rho)^2 \times 10^{-20}$, cm^{-4}
25	22.5	0.781	0.059
30	28.8	0.652	0.077
50	50.1	0.403	0.104

[a] For the parameter definitions, see the text and eqs 4 and 5.

These SANS results are consistent with our previous studies using pyrene as a hydrophobic probe, which showed that the F127−PAA−EGDMA microgels undergo a phase transition just below 25 °C.[17] In addition, these SANS results are analogous to those observed for solutions of the F127−PAA polymers that were not cross-linked by EDGMA.[13] In that study, micelles very similar in character to but somewhat larger than Pluronic micelles were observed when the temperature was increased above 15 °C and were responsible for gelation.[13] The phase behavior of the F127−PAA−EGDMA microgels appears to be very similar, in that, upon reaching the approximate micellization temperature of F127, the microgels undergo rearrangement of the PPO blocks to form hydrophobic domains on the nanometer scale. The spherical domains in the EGDMA-cross-linked microgels appear to be very polydisperse, which may be a result of the many cross-links that hinder rearrangement of the chains. In contrast to our observations with the F127−PAA polymer solutions,[13] the scattering increases into the USANS range for the F127−PAA−EGDMA microgels, suggesting that the micelle-like structures are cross-linked into a larger structure by EGDMA (i.e., the microgel particles).

The SANS behavior of the L92−PAA−EGDMA microgels is very different, in that no structural changes appear to take place on the nanometer scale upon heating (Figure 2b). Several attempts were made to fit the L92−PAA−EGDMA scattering data to models for polydisperse particles with interparticle interactions; however, none of the models was able to correctly capture all features of the data, most likely due to the strong interactions suggested by the sharply increasing scattering at low q values (of the SANS region). According to pyrene probe studies,[17] the L92−PAA−EGDMA microgel particles undergo a phase transition at ∼20 °C. However, unlike the F127−PAA−EGDMA microgel, there is no evidence from SANS that this involves a structural rearrangement at the nanometer scale because the scattering in this q range is essentially constant as the temperature is varied.

(30) Kotlarchyk, M.; Chen, S.-H. *J. Chem. Phys.* **1983**, *79*, 2461.
(31) Kotlarchyk, M.; Chen, S.-H.; Huang, J. S. *Phys. Rev. A* **1983**, *28*, 508.
(32) Schubel, D.; Bedford, O. D.; Ilgenfritz, G.; Eastoe, J.; Heenan, R. K. *Phys. Chem. Chem. Phys.* **1999**, *1*, 2521.
(33) Lee, C. T., Jr.; Psathas, P. A.; Ziegler, K. J.; Johnston, K. P.; Dai, H. J.; Cochran, H. D.; Melnichenko, Y. B.; Wignall, G. D. *J. Phys. Chem. B* **2000**, *104*, 11094.
(34) Feigen, L. A.; Svergun, D. I. *Structure Analysis by Small-Angle X-ray and Neutron Scattering*; Plenum Press: New York, 1987.

Like the F127−PAA−EGDMA microgel samples, the scattering continues to increase into the USANS range (Figure 2b), suggesting the aggregates are incorporated into a larger structure. The lack of nanoscale structural rearrangement may result from the higher degree of cross-linking in the L92−PAA−EGDMA microgels due to the higher PPO fraction in the polymer (see the discussion below).

USANS can provide information about the microgel structure in the 150 nm to 2.5 μm size range, thereby allowing a structural investigation of turbid systems that are not accessible to light scattering.[35] Since the swollen microgel particle size was on the order of tens of microns, USANS cannot give information about the total size. However, it can provide information about the structural arrangement of the nanometer size aggregates within the microgel particles. As shown in Figure 2a, the USANS data for the F127−PAA−EGDMA microgels are nearly constant as the temperature is varied between 10 and 50 °C, suggesting that the phase transition of these microgels is limited to nanometer scale rearrangement. A significant feature in the USANS region is the plateau centered at $\sim 8 \times 10^{-4}$ Å^{-1}, giving a characteristic length of $l = 2\pi/q = 0.8$ μm. This plateau could be a result of the large 1−2 μm pores observed by scanning electron microscopy (SEM) on the surface of the swollen F127−PAA−EGDMA microgel particles.[17] If the plateau is a result of the pores, the USANS results indicate that there is no significant change in the pore structure with temperature.

Analysis of the scattering in the USANS range for the L92−PAA−EGDMA microgels (Figure 2b) is complicated by the fact that there may have been structure in the 0.0044 Å$^{-1} < q < 0.0073$ Å^{-1} gap between the SANS and USANS measurements. SEM images of the swollen L92−PAA−EGDMA microgels indicated that these particles had a well-developed porous structure with a pore width of ~100 nm.[17] Scattering from these structures would be seen at $q \approx 6 \times 10^{-3}$, which lies in the gap between the SANS and USANS data. Any evidence of structure in this region is unfortunately obscured by the desmearing algorithm that forced a power law decay of the USANS data at high q values. Unlike the F127−PAA−EGDMA microgels, the L92−PAA−EGDMA microgels showed subtle differences with temperature in the USANS range, suggesting that the phase transitions of this material may involve structural changes in the 100 nm to 1 μm size range, which is very different from a typical micellization transition. The slope of the L92−PAA−EGDMA USANS data also provides information about the microgel structure. As shown in Figure 2b, the data at 25 °C approximately follow a $q^{-3.0}$ decay throughout the entire USANS range and into the SANS range. A q^{-D} scattering dependence can be explained by a fractal structure in which D is the fractal dimension.[36] A fractal dimension of 3.0 for the L92−PAA−EGDMA microgel at 25 °C suggests that the L92 microgels form a densely packed network of small aggregates, which is consistent with our observations using SEM.[17]

Differential Scanning Calorimetry Study. Typical thermograms of 1 wt % aqueous suspensions of microgels and 1 wt % solutions of the parent Pluronic are presented in Figure 4. All the observed effects were typical for other Pluronic solutions and microgel suspensions. The shown thermograms were obtained at a 1 K/min scanning rate,

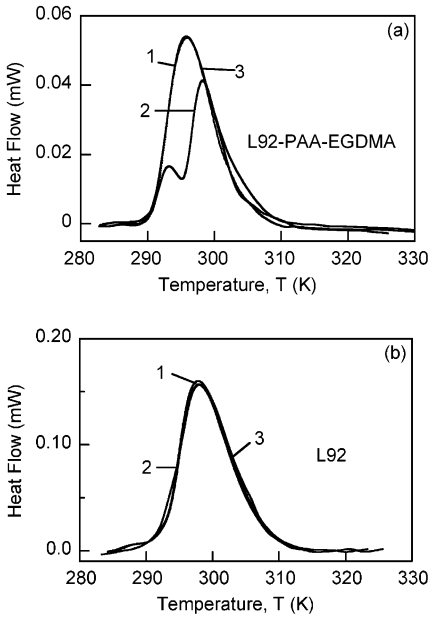

Figure 4. Three consecutive DSC heating scans of (a) a 1 wt % aqueous suspension of L92−PAA−EGDMA and (b) a 1 wt % solution of the parent Pluronic L92. Scanning rate, 1 K/min. The numbers indicate the number of the scan.

and the results of three consecutive heating scans are depicted. The instrumental raw data have the units of power (milliwatts). A heating scan was in each case followed by a brief (10 s) isotherm and by a cooling scan at the same rate. As is seen, pronounced endothermic peaks were observed in all cases, indicating cooperative transitions over a 10−20 K range. The Pluronic solution exhibited no significant differences between the first, second, and consecutive heating−cooling cycles (Figure 4b), which illustrates the complete reversibility of the transition, related to micellization of the polymer. Notably, in contrast to the Pluronic solutions, suspensions of microgels did show significant distinctions in the first and second heating−cooling scans, with the second heating endotherm typically split into two or more peaks. The reasons for such complex behavior may lie in slow structural changes in the microgel structure as dense, hydrophobic domains re-equilibrate at elevated temperatures.[13,16,17] However, these kinetically complicated changes disappeared in the third and consecutive scans, which always exhibited one superimposable peak. Since in this study we were interested only in the equilibrium properties of our systems, all the results described below were obtained using the results of the third scan, in which we observed mostly scan-rate-independent transitions in the microgel suspensions, as expected for systems that have reached equilibrium.[37,38] In some cases, there was a mismatch in the higher temperature range between the scans performed at different rates, but the results of the third heating cycle performed at the same heating rate were always identical.

Figure 5 shows the MSDSC heating thermograms obtained for microgels after two heating−cooling cycles. As is seen, a pronounced endothermic peak spanning 10−15 K corresponding to the aggregation transition was observed in all cases.

The SANS and USANS study described above demonstrated that nanosized domains in our microgels form in

(35) Kanaya, T.; Takeshita, H.; Nishikoji, Y.; Ohkura, M.; Nishida, K.; Kaji, K. *Supramol. Sci.* **1998**, *5*, 215.

(36) Hiemenz, P. C.; Rajagopalan, R. *Principles of Colloid and Surface Chemistry*, 3rd ed.; Marcel Dekker: New York, 1997.

(37) Sánchez-Ruiz, J.; López-Lacomba, J.; Cortijo, M.; Mateo, P. *Biochemistry* **1988**, *27*, 1648.

(38) Armstrong, J. K.; Chowdhry, B. Z.; Snowden, M. J.; Dong, J.; Leharne, S. A. *Thermochim. Acta* **2003**, *400*, 21.

Table 3. Transition Temperature (T_m), Entropy (ΔH), and Enthalpy (ΔS) of Aggregation for the F127−PAA−EGDMA (I) and L92−PAA−EGDMA (II) Microgels Obtained from Heat Capacity Thermograms at pH 7.0

	ΔH_{cal},[a] J g^{-1}		ΔS_{cal},[a] J g^{-1} K^{-1}		ΔH_{vH},[b] kJ mol^{-1}		ΔH^*,[c] kJ mol^{-1}	
C, wt %	I	II	I	II	I	II	I	II
1.0	11.6	17.9	0.039	0.060	348.9	362.5	324.1	147.5
2.0	12.5	17.0	0.043	0.057	345.1	385.2	350.6	140.7
3.0	12.5	15.5	0.042	0.052	349.8	383.5	350.3	127.8
4.0	12.2	17.8	0.042	0.060	355.7	382.9	341.3	147.2
5.0	12.0	16.8	0.041	0.057	366.3	416.4	334.8	139.0
7.5	12.2	17.4	0.042	0.059	371.1	420.4	341.6	143.4

[a] The data are calculated per gram of dry network. The calorimetric ΔH_{cal} and ΔS_{cal} values are obtained from the integrated area under the C_p versus T or C_p versus ln T curves, respectively, as explained in the Experimental Section. [b] The van't Hoff enthalpy (ΔH_{vH}) is calculated from the experimental C_p versus T thermograms (Figure 5) using eq 7. [c] The ΔH^* values are calculated per mole of Pluronic in the dry network, given a weight fraction of the Pluronic in the copolymer of 0.45 and assuming the molecular masses of the F127 and L92 segments bonded into the network to be 12 600 and 3720 g/mol, respectively.

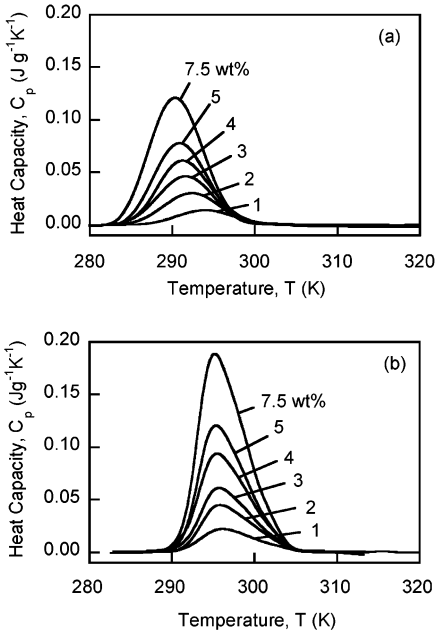

Figure 5. Experimental heat capacity (C_p) thermograms for 1.0−7.5 wt % aqueous microgel suspensions (pH 7.0) of the (a) F127−PAA−EGDMA and (b) L92−PAA−EGDMA microgels. A linear baseline correction was applied to all of the thermograms. Underlying heating rate, 0.0167 K/s; amplitude, ±0.16 K; frequency, 0.1 rad/s.

aqueous suspensions at elevated temperatures. Such aggregation is caused by the temperature sensitivity of the aqueous solubility of the PPO segments of the Pluronic bonded into the microgel network. Much like the un-cross-linked Pluronic−PAA polymers, which can form intra- and intermolecular micelle-like aggregates because of the hydrophobic interactions,[12] the microgels can form aggregates. The DSC endotherms show that the process of aggregation is reversible and endothermic upon heating. In the present work, we set out to evaluate the thermodynamics of such aggregation and compare the results with the parameters of aggregation of Pluronics.

On the basis of the DSC method, the enthalpy of micellization of the Pluronic F127 aqueous solutions was reported to range from 161 to 366 kJ mol^{-1}, depending on concentration,[39−43] while the entropy was reported to be ΔS_{mic} = 0.67 kJ mol^{-1} K^{-1}.[39] We are unaware of any literature data on the ΔH_{mic} values of the Pluronic L92 in water. The poly(propylene oxide) (MW, 1000 g/mol) possesses a ΔH_{agg} value of 103−143 kJ mol^{-1}.[38]

A strong correlation has been reported between the composition of Pluronics and the enthalpy of their micellization in water:[40]

$$\Delta H_{agg} = 117.6 - 0.187N_{EO} + 3.25N_{PO} \qquad (6)$$

where N_{EO} and N_{PO} are the numbers of ethylene oxide and propylene oxide units, respectively. Notably, the number of PO units dominates the expression (eq 6), which is mechanistically rationalized in terms of the key role of the PO units, which undergo dehydration, in the aggregation process. Equation 6 yields estimates of ΔH_{mic} for the Pluronics L92 ($EO_8PO_{52}EO_8$) and F127 ($EO_{99}PO_{67}EO_{99}$) to be 283.6 and 298.3 kJ mol^{-1}, respectively. Our own measurements of aqueous solutions of the Pluronics in the concentration range 1−5 wt % yielded 265−300 and 270−310 kJ mol^{-1} for the solutions of L92 and F127, respectively, in a good agreement with these estimates and the literature data.

The thermodynamic parameters of the microgels having respective Pluronic copolymers bonded to the PAA segments are collected in Table 3. Positive changes in both enthalpy and entropy upon aggregation are typical for entropy-driven aggregation processes due to hydrophobic associations.[25,44]

The van't Hoff enthalpy (ΔH_{vH}) was calculated from the respective thermograms using the relation[45,46]

$$\Delta H_{vH} = \frac{4RT_m^2\Delta C_p^{tr}(T_m)}{\Delta H_{cal}} \qquad (7)$$

where ΔC_p^{tr} is the experimental transition heat capacity function (Figure 5), T_m is the temperature at which the excess heat capacity function has a maximum, and R = 8.314 J mol^{-1} K^{-1} is the universal gas constant.

It is interesting to observe that the F127−PAA−EGDMA microgels exhibited a ΔH^* value (calculated *per mole of Pluronic* from ΔH_{cal}) close to that of the parent Pluronic in water and in excellent agreement with the van't Hoff enthalpy (ΔH_{vH}). The ΔH_{vH} values are obtained from the experimental thermograms, without any a priori

(39) Paterson, I.; Armstrong, J.; Chowdhry, B.; Leharne, S. *Langmuir* **1997**, *13*, 2219.
(40) Beezer, A. E.; Loh, W.; Mitchell, J. C.; Royall, P. G.; Smith, D. O.; Tute, M. S.; Armstrong, J. K.; Chowdhry, B. Z.; Leharne, S. A.; Eagland, D.; Crowther, N. J. *Langmuir* **1994**, *10*, 4001.
(41) Mitchard, N. M.; Beezer, A. E.; Mitchell, J. C.; Armstrong, J. K.; Chowdhry, B. Z.; Leharne, S.; Buckton, G. *J. Phys. Chem.* **1992**, *96*, 9507.
(42) da Silva, R. C.; Olofson, G.; Schillen, K.; Loh, W. *J. Phys. Chem. B* **2002**, *106*, 1239.
(43) Alexandridis, P.; Holzwarth, J. F.; Hatton, T. A. *Macromolecules* **1994**, *27*, 2414.
(44) Tanford, C. *The Hydrophobic Effect: Formation of Micelles and Biological Membranes*; John Wiley: New York, 1980.
(45) Privalov, P. L. *Adv. Protein Chem.* **1979**, *33*, 167.
(46) Haynie, D. T.; Freire, E. *Anal. Biochem.* **1994**, *216*, 33.

assumptions regarding the molecular weights of the aggregating species. The close values of ΔH^* and ΔH_{vH} are evidence of the two-state transition.[47,48] However, the enthalpy of aggregation (ΔH^*) of the L92−PAA−EGDMA microgels was 2.5−3-fold less than the corresponding ΔH_{vH} values. The standard error of the ΔH^* determination measured in three independent tests was below 5%. To calculate ΔH^* here, the original molecular masses of the parent Pluronics were applied. The above results can be rationalized by the change in the length of the PPO segments bonded in the polymer structure as follows.

Synthesis of the Pluronic−PAA microgels involves free-radical polymerization of acrylic acid

$$R\bullet + nAA \rightarrow R{-}AA_n\bullet$$

with the chain transfer to the Pluronic via hydrogen abstraction resulting in C−C bonding between the PAA chains and the Pluronic:[7,10,14]

$$R\bullet + X_mH \rightarrow RH + X_m\bullet$$

$$R{-}AA_n\bullet + X_mH \rightarrow R{-}AA_nH + X_m\bullet$$

$$X_m\bullet + pAA \rightarrow X_m{-}AA_p\bullet$$

where R• is the free radical, X_mH is the Pluronic, and AA is the acrylic acid monomer. One Pluronic−PAA molecule contains numerous PAA and Pluronic segments. Importantly, the abundance of Pluronic macroradicals can result in their recombination:

$$X_m\bullet + X_m\bullet \rightarrow X_m{-}X_m$$

The Pluronic homopolymers and gels generated in this way can be subject to further hydrogen abstraction reactions and thus to grafting of additional PAA chains. If driven to completion, the polymerization leads to the appearance of gels that possess nanosized clusters that are more hydrophobic than the original Pluronics.[14] We have reported previously,[15,16] that because of the higher propensity of the PPO segments to undergo hydrogen abstraction in the process of the microgel synthesis, the microgels with the lower PO content will have fewer PAA segments grafted onto one PPO chain. In the F127−PAA−EGDMA microgels, where Pluronic segments are bonded to the PAA network rather loosely, the Pluronic segments will have sufficient flexibility to aggregate as flexible dangling chains. Conversely, the microgels with higher PPO content will have a higher density of the PAA segments covalently bonded to the Pluronic backbones. Moreover, since PAA segments link Pluronic segments into a graft-comb structure,[14] densely grafted PPO segments belonging to different Pluronic macromolecules will be linked by several PAA segments, effectively creating larger clusters aggregating together as entities larger than single Pluronic segments. In order for the ΔH^* value to be equal to the ΔH_{vH} value in the L92−PAA−EGDMA networks, these networks should have aggregating species with an effective molecular weight 2.5−3-fold larger than that of a single Pluronic L92 chain (Table 3). This conclusion is consistent with the high PPO content and the abundance of cross-linked clusters in these networks.[15,16] Our SANS results also indicate a fractal structure formed from small cross-linked clusters.[34]

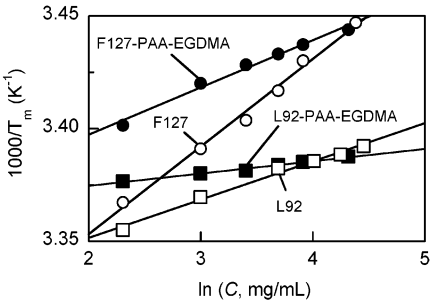

Figure 6. Correlation between the aggregation peak maximum (T_m) and the total polymer concentration (C, mg/mL) in the microgel suspensions (filled points) and the Pluronic solutions (open points). The solid lines represent linear fits.

Table 4. Apparent Standard Enthalpy (ΔH_0^*) and Free Energy (ΔG_0^*) of Aggregation Obtained from the Concentration Dependencies of T_m Measured in Aqueous Microgel Suspensions or Solutions of Pluronic Copolymers

species	ΔH_0^*, kJ mol^{-1}	ΔG_0^*,[a] kJ mol^{-1}
L92−PAA−EGDMA	1667.2 ± 750.3	−30.7 ± 1.79
L92	559.6 ± 177.2	−14.05 ± 5.1
F127−PAA−EGDMA	434.7 ± 79.9	−33.3 ± 1.88
F127	212.3 ± 51.5	−14.63 ± 1.9

[a] The ΔG_0^* values are calculated per mole of Pluronic in solution or suspension, assuming the molecular masses of the F127 and L92 segments bonded into the network to be 12 600 and 3720 g/mol, respectively.

Considering aggregation as a multimeric temperature-induced reaction and following the well-known analysis applied to Pluronic solutions,[43,49,50] we can relate the apparent standard enthalpy of aggregation (ΔH_0^*) to the characteristic temperature (T^*) taken as a critical aggregation temperature[49,50] or, equivalently,[51] as the temperature of the maximum of the C_p peak due to aggregation (T_m) via the Gibbs−Helmholz equation:

$$\left[\frac{\partial(1/T_m)}{\partial \ln C}\right] = \frac{R}{\Delta H_0^*} \qquad (8)$$

Here, C is the total polymer concentration in the suspension or the solution. Equation 8 predicts that ln C should vary linearly with the reciprocal of T_m with a slope of $\Delta H_0^*/R$. Figure 6 shows the T_m values determined experimentally for solutions of Pluronics as well as aqueous microgel suspensions as functions of the total polymer concentration (C) in terms of eq 8. The linear regressions fit the data well, with $R^2 > 0.98$ in all cases.

The values of the apparent standard enthalpy of aggregation (ΔH_0^*) were calculated using the slopes of the linear fits (Figure 6) and are collected in Table 4. The values of the apparent free energy of aggregation (ΔG_0^*) were calculated from the expression[49]

$$\Delta G_0^* = RT_m \ln C' \qquad (9)$$

where C' (moles per liter) is the effective Pluronic concentration in the corresponding polymer solution or microgel suspension.

(47) Privalov, P. L. *Adv. Protein Chem.* **1979**, *33*, 167.
(48) Sturtevant, J. M. *Annu. Rev. Phys. Chem.* **1987**, *38*, 463.
(49) Deng, Y.; Yu, G.-E.; Price, C.; Booth, C. *J. Chem. Soc., Faraday Trans.* **1992**, *88*, 1441.
(50) Booth, C.; Attwood, D. *Macromol. Rapid Commun.* **2000**, *21*, 501.
(51) Tamura, A.; Privalov, P. L. *J. Mol. Biol.* **1997**, *273*, 1048.

The negative ΔG_0^* values show that aggregation is a thermodynamically favored process. In the case of the Pluronic F127 and L92 solutions, the values of the apparent standard enthalpy change in Table 3 correspond quite well with the literature estimates for the Pluronic F127 and L92 solutions of 253 and 550 kJ mol^{-1}, respectively,[49,52] obtained either by DSC or probe solubilization techniques.[50,52] The ΔH_{vH} and ΔH^* values obtained from the DSC thermograms are related to, but typically do not coincide with, the ΔH_0^* values.[49,50] The ΔH_0^* values are 2−3-fold higher for the microgels than for the solutions of their respective Pluronic solutions, showing that T_m for the microgels was much less concentration-dependent than it was in the Pluronic solutions. This pronounced effect can be explained by the high concentration of hydrophobic domains that exist in the microgels below their critical aggregation temperatures, and thus are exposed to water before the start of the aggregation, maximizing the structuring of the water (i.e., the hydrophobic effect).[13,16,17] The spectra of the polarity-sensitive fluorescence probe, pyrene, indicate that such domains consist of Pluronic−PAA clusters that appear to be much more nonpolar and hydrophobic than the corresponding Pluronic or even PPO aggregates.[17] Transfer of such small hydrophobic clusters into the hydrophobic core of the micelle-like aggregate involves a large enthalpy change, as is seen from our results.

Microgel Swelling Study. To evaluate the thermodynamics of microgel swelling, we apply the classic Flory theory,[53,54] wherein the Helmholtz free energy of a gel is the sum of the free energies of the solvent and the amorphous polymer, the mixing free energy, and the elastic free energy of the gel network. The gel reaches equilibrium when its total osmotic pressure (π) vanishes. Considering contributions to the osmotic pressure of the mixing free energy (π_m), the elastic free energy (π_{el}), and the Donnan-type potential (π_{ion}),[54] the condition of equilibrium can be written as

$$\pi = \pi_{el} + \pi_m + \pi_{ion} = 0 \tag{10}$$

where the osmotic pressure contributions per gel unit volume (a^3) are functions of the polymer volume fraction (ϕ):

$$\pi_m = -\frac{k_B T}{a^3}[\phi + \ln(1-\phi) + \chi\phi^2] \tag{11}$$

$$\pi_{el} = \frac{k_B T}{a^3}\frac{\phi_0}{N_x}\left[0.5\left(\frac{\phi}{\phi_0}\right) - \left(\frac{\phi}{\phi_0}\right)^{1/3}\right] \tag{12}$$

$$\pi_{ion} = \frac{k_B T}{a^3}\frac{\phi_0 f}{N_x}\left(\frac{\phi}{\phi_0}\right) \tag{13}$$

Herein, ϕ_0 is the polymer volume fraction at the reference state, N_x is the length of the subchain (commonly defined as the degree of polymerization between cross-links), f is the average number of ionized monomers between cross-links, χ is the Flory interaction parameter, and $k_B = 1.38 \times 10^{-23}$ J K^{-1} is the Boltzmann constant.

It must be noted that the reference state in our case will be the state of a gel equilibrium swollen at an arbitrarily chosen (low) temperature, rather than the state of the "as synthesized" gel.

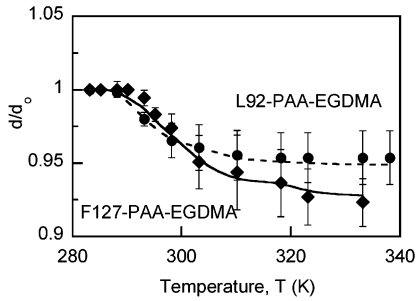

Figure 7. Equilibrium swelling of microgels as a function of temperature at pH 7.0. The experimental data and regressed fits are shown by points and solid (F127−PAA−EGDMA) or dashed (L92−PAA−EGDMA) lines, respectively. The diameter of each gel particle at 10 °C was chosen as a reference (d_0). Each datum point represents an average ± SD of five independent measurements. See the text for more details.

Combining eqs 10−13 and rearranging, we obtain

$$\frac{\phi_0}{N_x}\left[0.5\left(\frac{\phi}{\phi_0}\right) - \left(\frac{\phi}{\phi_0}\right)^{1/3}\right] + \frac{\phi_0 f}{N_x}\left(\frac{\phi}{\phi_0}\right) - \phi + \ln(1-\phi) + \chi\phi^2 = q(\phi, T) = 0 \tag{14}$$

The gel volume fractions at the swelling equilibrium and at the reference state (ϕ and ϕ_0, respectively) are related to the respective gel diameters.

$$\phi_0/\phi = (d/d_0)^3 \tag{15}$$

The interaction parameter is temperature-dependent and at a fixed ϕ value can be expanded[55−57] in a power series as

$$\chi_1(T, \phi) = \chi_1 + \chi_2\phi + \chi_3\phi^2 + \ldots \tag{16}$$

Following a widely applied assumption[55] that χ_1 is temperature-dependent and χ_2 is a constant, eq 16 can be simplified to

$$\chi = \chi_1(T) + \chi_2\phi \tag{17}$$

Herein, χ_1 can be expressed via the enthalpy (ΔH_m, J) and entropy (ΔS_m, J K^{-1}) *per mole* of the monomeric units of the network:

$$\chi_1 = (\Delta H_m - T\Delta S_m)/k_B T \tag{18}$$

Using experimentally measured temperature dependencies of the equilibrium gel diameter, we applied eqs 14−18 to relate structural parameters of our microgels to their thermodynamic characteristics obtained by DSC.

Figure 7 shows the relative diameters of the microgels equilibrium swollen at each respective temperature. The reference state (d_0) of the microgels was chosen to be the one at 10 °C, because this temperature is below the range where the endothermic aggregation within microgel particles takes place, and thus, the network structure is less perturbed. As is seen, the diameter of the microgels decreases with temperature, consistent with the appearance of additional cross-linking because of the aggregation. The lines in Figure 7 represent the optimum fit of the model to the experimental swelling data, in which the

(52) Paterson, I. F.; Chowdhry, B. Z.; Leharne, S. A. *Langmuir* **1999**, *15*, 6187.
(53) Flory, P. J. *Principles of Polymer Chemistry*; Cornell University Press: Ithaca, NY, 1957.
(54) Shibayama, M.; Tanaka, T. *Adv. Polym. Sci.* **1993**, *109*, 1−62.
(55) Erman, B.; Flory, P. J. *Macromolecules* **1986**, *19*, 2342.
(56) Orofino, T. A.; Flory, P. J. *J. Chem. Phys.* **1957**, *26*, 1067.
(57) Hirotsu, S. *J. Chem. Phys.* **1991**, *94*, 3949.

Table 5. Thermodynamic and Structural Parameters Used in Computation of the Temperature Dependence of Microgel Swelling

parameter	microgel: L92−PAA−EGDMA	microgel: F127−PAA−EGDMA
total amount of monomers per gram of dry network,[a] mmol	15.94	16.13
ΔH,[b] kJ mol^{-1}	1.07 ± 0.055	0.74 ± 0.038
ΔS,[b] J mol^{-1} K^{-1}	3.60 ± 0.19	2.54 ± 0.13
ΔH_m,[c] J	-1.78×10^{-21}	-1.23×10^{-21}
ΔS_m,[c] J K^{-1}	-5.99×10^{-24}	-4.21×10^{-24}
polymer volume fraction at the reference state (ϕ_0)[d]	0.035 ± 0.0032	0.025 ± 0.0045

[a] In calculation of the total amount of monomers, the number average weight of the EO and PO units was taken as 54.7 and 47.5 g/mol for the Pluronics L92 and F127, respectively. The alkylene oxide units are capable of hydrogen abstraction and of generating radicals in the process of the synthesis[7,10,14] and thus are treated as monomers in our case. [b] The data are calculated *per mole of monomer* total present in the network. The average of six independent measurements ± SD is shown. [c] To obtain absolute values of ΔH_m and ΔS_m, the average ΔH and ΔS values were divided by $N_A = 6.02 \times 10^{23}$. The negative sign was assigned to both the enthalpy and entropy changes, since the process of the gel swelling upon cooling is exothermic, while the collapse upon heating is endothermic. [d] The polymer volume fraction was measured using a microscopic technique.[16,17] The diameter of a dry microgel particle (d_d) was measured, and then the particle was immersed in water at 10 °C, pH 7.0, and was allowed to equilibrium swell, yielding the swollen diameter (d_t). The ϕ_0 value was calculated as $(d_t/d_d)^3$. The listed numbers represent averages ± SD of five independent measurements. In computation, only the average d/d_0 values at each temperature were used.

model parameters N_x, f, and χ_2 were extracted by nonlinear least squares regression by minimizing the sum of square residuals (see eq 14):

$$Q = \sum_i^n [q_i(\phi_i, T_i)]^2 \qquad (19)$$

where ϕ_i is the gel volume fraction at a given temperature, T_i. In the computation, ΔH_m and ΔS_m were fixed at the values listed in Table 5.

Because the L92−PAA−EGDMA microgels are more hydrophobic than F127−PAA−EGDMA, their ionization starts at a significantly higher pH (Table 1). On the basis of the intrinsic dissociation constants (pK_0's) of the L92−PAA−EGDMA and F127−PAA−EGDMA microgels found from potentiometric titration to be 6.27 and 4.95, respectively (Table 1), one can see that at pH 7.0 all of the carboxyls available for titration in the F127−PAA−EGDMA microgels are ionized, while only ∼40% of such carboxyls are ionized in the L92−PAA−EGDMA microgels. These estimates together with the ∼1:1 molar ratio of the acrylic acid to ether units in the network yield the number of ionized monomers (f) to be $\sim 0.2N_x$ and $\sim 0.4N_x$ in the L92−PAA−EGDMA and F127−PAA−EGDMA microgels, respectively. The optimal values of f extracted from the curve-fitting of the model to the experimental swelling data were at least 2-fold lower than these estimates. Such a result is commonly observed in heterogeneous polyelectrolyte gels and is explained by the trapping of the counterions in the gel inhomogeneities as well as by the Manning condensation on the line of charges.[58,59] The physical meaning of an f value lower than that estimated from the titration data is the lower relative number of osmotically active counterions that contribute to the osmotic swelling, since these counterions can be trapped in the dense, hydrophobic domains observed in our Pluronic−PAA systems.[13,16]

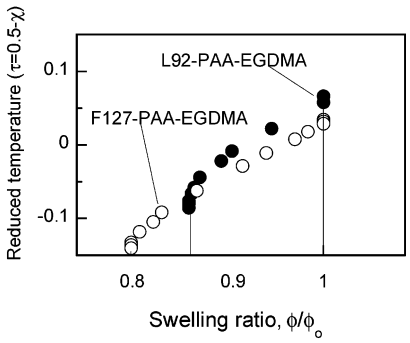

Figure 8. Swelling phase diagram of microgels in terms of the reduced temperature ($\tau = 0.5 - \chi$) vs degree of swelling (ϕ/ϕ_0). The Flory interaction parameter (χ) applied in the phase diagram was calculated from the d/d_0 values. The vertical lines indicate the fully swollen and collapsed equilibrium states of the microgels. The degree of swelling is obtained from the experimental microgel diameter data: $\phi/\phi_0 = (d/d_0)^3$.

The inhomogeneities and entanglements contribute to the higher ϕ_0 value (i.e., the lower swelling degree) in the case of the more inhomogeneous and less charged L92−PAA−EGDMA microgels. The presence of inhomogeneities such as polymer-rich, dense domains in polyelectrolyte gels allows for the predictions[58] that the inhomogeneous gel is less swollen than its homogeneous counterpart and that the higher the gel charge, the lower the swelling of the gel in comparison to its homogeneous analogue.

The model fitting utilizing experimentally obtained ΔH_m and ΔS_m values yielded the model Flory interaction parameter (χ). The χ values increased above the aggregation temperatures, a manifestation of the worsening of the solvent,[54,60−62] and mimicked the temperature-induced volume phase transition in gels. Following Tanaka et al.,[54,63] we constructed a phase diagram of our microgels in reduced temperature ($\tau = 0.5 - \chi$) versus the degree of swelling coordinates (Figure 8).

The transition in the more ionized F127−PAA−EGDMA microgels started at a lower τ value, and the region between the fully swollen and collapsed states (designated by vertical lines) was wider in the case of the F127−PAA−EGDMA microgel. Both of these trends are expected, given the higher onset temperature and higher extent (d/d_0 change) of the temperature-induced transition with microgels of this type. The depicted phase diagram supports the validity of our model and is fundamentally analogous to the one built for the gels of poly(*N*-isopropylacrylamide-*co*-acrylic acid).[64] The region between fully swollen and collapsed states in the latter gels, as in our case, widens with the degree of ionization. The absence of a discontinuous phase transition, which would be manifested by a horizontal line connecting swollen and collapsed ϕ/ϕ_0 values in Figure 8, can be explained by the polydispersity of the PPO aggregates acting as cross-links. As indicated by the quite broad endothermic aggregation peaks (Figure 5), these aggregates exhibit a range of critical aggregation temperatures, rather than a single

(58) Zeldovich, K. B.; Khokhlov, A. R. *Macromolecules* **1999**, *32*, 3488.
(59) Manning, G. S. *Annu. Rev. Phys. Chem.* **1972**, *23*, 117.
(60) Flory, P. J. *J. Chem. Phys.* **1949**, *17*, 223.
(61) Huggins, M. L. *Ann. N. Y. Acad. Sci.* **1943**, *44*, 431.
(62) Flory, P. J.; Knigbaum, W. R. *Annu. Rev. Phys. Chem.* **1957**, *2*, 383.
(63) Tanaka, T.; Fillmore, D. J.; Sun, S.-T.; Nishio, I.; Swislow, G.; Shah, A. *Phys. Rev. Lett.* **1980**, *45*, 1636.
(64) Hirotsu, S.; Hirokawa, Y.; Tanaka, T. *J. Chem. Phys.* **1984**, *87*, 1392.

lower critical solution temperature as in the case of the poly(*N*-isopropylacrylamide-*co*-acrylic acid) gels that show discontinuous volume phase transitions.

Concluding Remarks

Neutron scattering, DSC, and equilibrium swelling experiments have been conducted on microgels comprising PAA networks to which Pluronic PEO−PPO−PEO copolymers are covalently bonded. The microgels exhibit thermodynamically favorable volume phase transitions within certain temperature ranges due to reversible intraparticle aggregation of the PPO chains, which occurs because of hydrophobic associations. Comparison of the apparent standard enthalpy of aggregation (ΔH_0^*) in the microgel suspensions with that in the solutions of parent Pluronics revealed a ΔH_0^* value 2−3-fold higher in microgel suspensions, indicating that the hydrophobic clusters present in the microgels rearrange at the temperature of aggregation, assembling into supramolecular structures. Such hydrophobic clusters that represent dense, cross-linked domains in the microgels have been shown to be more hydrophobic than un-cross-linked PPO chains.[13,16,17]

To attenuate the effects of the hydrophobicity of the Pluronic incorporated into the microgel structure, we developed microgels based on PAA and either the hydrophobic Pluronic L92 (PPO content, 80%) or the hydrophilic Pluronic F127 (PPO content, 30%). Neutron scattering indicates formation of micelle-like aggregates within the F127−PAA−EGDMA microgels, while the L92−PAA−EGDMA microgels form a fractal network of nanometer size clusters. It also appears that incorporation of different Pluronics alters significantly the swelling and aggregation behavior of the microgels. Thus, the F127−PAA−EGDMA microgels exhibited an enthalpy change upon aggregation close to that of the parent Pluronic in water and in excellent agreement with the van't Hoff enthalpy. However, the enthalpy of aggregation of the more hydrophobic L92−PAA−EGDMA microgels was 2.5−3-fold less than the corresponding van't Hoff enthalpy. Together with the neutron scattering data, these differences demonstrate that in the F127−PAA−EGDMA microgels dangling Pluronic chains possess enough steric freedom to aggregate in a fashion similar to that in Pluronic solutions, while in the L92−PAA−EGDMA microgels aggregation is mostly due to the assembly of hydrophobic domains rather than individual chains.

To summarize our equilibrium swelling results, we have observed a less pronounced temperature dependence and lower swelling degree in the case of the L92−PAA−EGDMA microgels, which are more inhomogeneous[17] than their F127−PAA−EGDMA analogues. The temperature dependence of the swelling degree appears to agree qualitatively with the classic theory of volume phase transitions in gels.[54] Notably, the microgels appear to have more effective cross-links than what can be estimated on the basis of the ratio of the divinyl cross-linker EGDMA to the monomers set in the synthesis. This conclusion correlates well with the microstructure of our microgels observed by using small- and ultra-small-angle neutron scattering techniques.

Acknowledgment. This work was accomplished with the financial support from the Cambridge-MIT Institute and the Singapore-MIT Alliance. We acknowledge the support of the National Institute of Standards and Technology, U.S. Department of Commerce, in providing the neutron research facilities used in this work (USANS). This work utilized facilities supported in part by the National Science Foundation under Agreement No. DMR-9986442. The authors would like to thank John Barker and Man-Ho Kim of NIST for their assistance in planning and executing the USANS experiments. We also acknowledge the support of the ISIS Pulsed Neutron & Muon Source for providing the neutron facilities for the SANS experiments performed in this work. The authors would like to thank Richard Heenan of ISIS and Julian Eastoe for their assistance with the SANS experiments.

LA0359530